The design of flux concentrated type transverse flux cylindrical PMLSM for high thrust

Shin Jung-Seob[1], Takafumi Koseki[1], Kim Houng-Joong[2]

[1]The University of Tokyo, Engineering Building #2 12F, 7-3-1 Hongo Bunkyo-ku, Tokyo 113-8656, Japan
[2] Sung-Jin Royal Motion Co. Ltd, 103-1311, Digital Empire 2, Sin-dong 486,
Yeongtong-gu, Suwon-si, Gyeonggi-do, 443-734, Korea
Email: Jungseobshin1008@koseki.t.u-tokyo.ac.jp

ABSTRACT

Linear motors have been attracting a great interest from industries these days for their fast and precise control capability. However, conventional single-sided linear motors have serious engineering problems. One of these disadvantages is the normal attractive magnetic force between an armature core and field magnets. The authors proposed a novel flux concentrated type transverse flux cylindrical PMLSM using generic armature cores for rotary machinery to cancel the normal attractive magnetic force and gain higher thrust. In this paper, a basic structure and the operational principle of the proposed cylindrical linear motor are described.

1 INTRODUCTION

Linear motors have been attracting a great interest from industries these days for their fast and precise control capability. Such direct devices offer many advantages over ball-skrew drive, notably the absence of mechanical gears and transmission systems, which results in a higher dynamic performance and reliability.

There are many types of linear motors including linear synchronous motor, linear induction motor and linear stepping motor etc. Especially, linear synchronous motor that uses permanent magnets (PMLSM) in the field side has contributed to the popularization in industrial fields.

In general, characteristics required to PMLSM in industrial fields are high thrust, high positioning accuracy and simple structure etc. Among these characteristics, high thrust can be an important technical requirement to PMLSM when considering conveyance of heavy materials such as large glasses.

The authors propose flux concentrated type transverse flux cylindrical PMLSM for high thrust. In this paper, a basic structure and the operational principle of the proposed model are described. Also, concept of flux concentrated type field for high thrust is introduced and its characteristics are both theoretically analyzed and numerically computed using finite element method (FEM).

2 BASIC STRUCTURE AND THE OPERATIONAL PRINCIPLE OF THE PROPOSED MOTOR

2.1 Point of new motor design

In design, the authors considered main points as below.

(1) High thrust, compact size, simple structure
(2) Low detent force
(3) Simple compatibility with conventional ball-skrew actuators
(4) Large 2nd moment of area, high bending stiffness
(5) Easy design and production
(6) Structurally compensated the normal attractive force

The authors decided to choose cylindrical shape from (3) and (4) and use generic armature cores for rotary machinery from (5) and (6).

2.2 Basic structure and the operational principle in the basic model

In the basic model, generic armature cores of brushless DC motor are used in the armature side (mover). One armature core has four salient poles and armature coils are wound around each salient pole as shown in Fig. 1(a).

Since generic armature cores for rotary machinery are used in the armature side, it is not necessary to consider new shape of armature core in the stage of new motor design. Hence, time and a burden to design a shape can be saved.

In addition, the strong normal force between armature and field sides is inherently compensated in the cross-sectional symmetrical closed magnetic form of the magnetic circuits identical to rotary machinery.

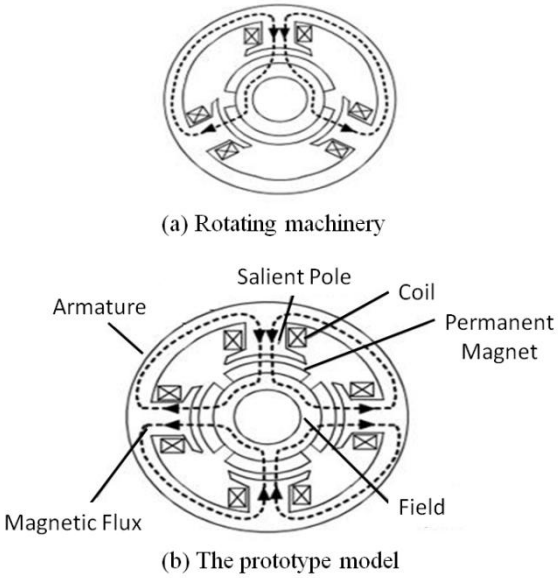

Figure 1: Fundamental configuration of three-phase armature units of the basic model

The magnet arrays also consist of cylindrical parts as illustrated in Fig. 2. This cylindrical structure realizes relatively large second moment of area, *i.e.*, the cylindrical field side is mechanically robust to bending external force. Consequently, mechanical support of the proposed linear motor is inherently simple.

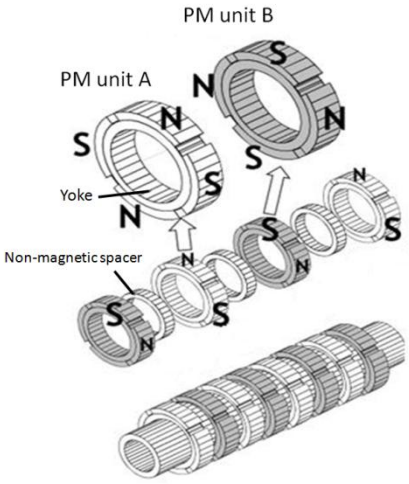

Figure 2 : Fundamental configuration of field magnet units of the basic model

Also, deflection is one of disadvantages in cylindrical PMLSM. Hence, achieving long stroke in cylindrical structure is generally difficult because the field side is fixed in both ends. In the proposed model, long stroke can be achieved by cutting one portion in the armature side and inserting supporting mechanism to its cutting space as shown in Fig. 3.

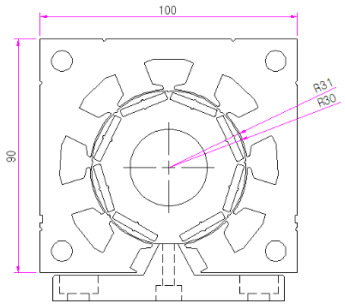

Figure 3 : Open type model for long stroke

3 THE PROPOSAL OF FLUX-CONCENTRATED FIELD FOR HIGHER THRUST

The typical method to obtain higher thrust by concentrating flux to the air gap is Halbach array. In Halbach array, high thrust can be obtained by changing the direction of magnetization.

However, using Halbach array in the basic model is not relatively effective because strong adhesive and equipment to attach and fix magnets are needed. This results in an increasing cost and can be a burden in the manufacturing stage. For that reason, the authors propose a new method of concentrating flux to the air gap. This concept is shown in Fig. 4.

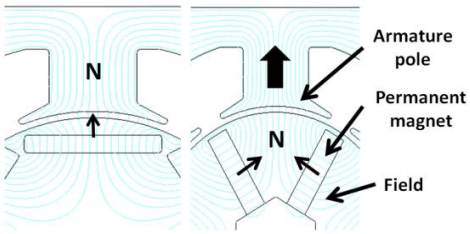

(a) The basic configuration (b) The flux-concentration configuration

Figure 4: The concept of flux concentration.

The concept of flux-concentration is relatively simple. In the basic configuration, one permanent magnet makes one magnetic pole in PMLSM as shown in Fig. 4(a). The authors thought that flux could be concentrated to the air gap as simple form when magnets with same magnetic pole are faced each other. In other words, one magnetic pole can be made by two magnets. By facing each other, magnetic field lines from each magnet are concentrated in the field side and then they pass through the air gap and the armature side as shown in Fig. 4(b). Hence, higher thrust can be obtained.

If this concept can be realized, higher thrust could be obtained using the same amount of the magnet or less than the proposed model with the basic configuration. Also, strong adhesive and equipment to attach or fix magnets are not needed because it is enough to insert magnets in holes of laminated steel plate. For that reason, low manufacturing cost and easy production will be achieved.

To verify the effectiveness of the idea of flux concentration, the authors applied two-dimensional FEM field calculation to the cross-section of the basic configuration and the flux-concentration configuration. In order to obtain the effect of flux-concentration, the authors choose six armature poles in the one armature side. One of the results is shown in Fig. 5.

The maximum flux density in the air gap increased to 0.902T in comparison with the reference model which the maximum air gap flux density is 0.734T in the case of using the same amount of the magnet as shown in Fig. 5(b). This is increase of 22.89%. Also, the maximum flux density in the armature pole increased to 1.39T in comparison with the reference model which the maximum flux density in the armature pole is 1.168T as shown in Fig. 5(c). This is increase of 18.74%. For that reason, the possibility of high thrust is verified through the proposed idea.

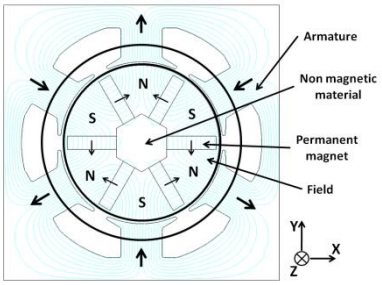

(a) Flux distribution

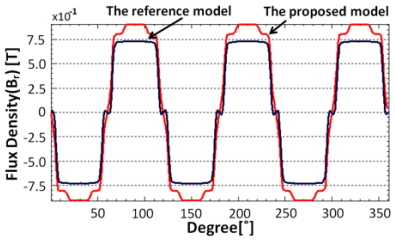

(b) Air gap flux density
(Marked as circle on the armature side in Fig. 5(a).)

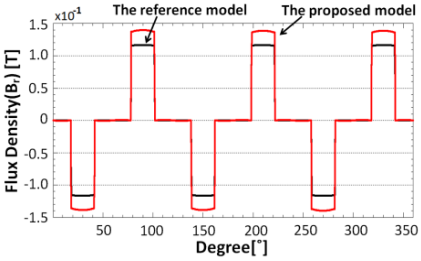

(c) Flux density in armature
(Marked as circle on the air gap in Fig. 5(a).)

Figure 5: Flux distribution of the cross-section and flux density of air gap and armature pole in the proposed model.

The fundamental configuration of three-phase units of the proposed model is shown in Fig. 6. The distance between point Z1 and point Z2 shown in Fig. 6(b) is one mechanical period in the moving direction. Also, the distance between point Y1 and point Y2 shown in Fig. 6(c) is the length of non-magnetic material spacer in the y-direction.

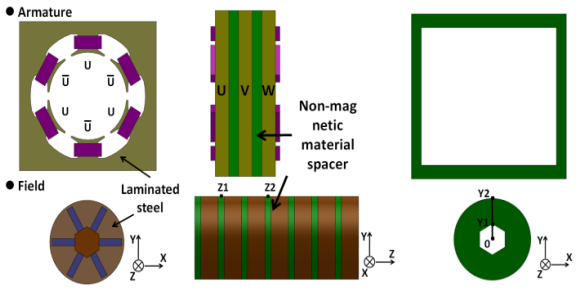

(a) The front side (b) The moving direction side (c) Non-magnetic material spacer

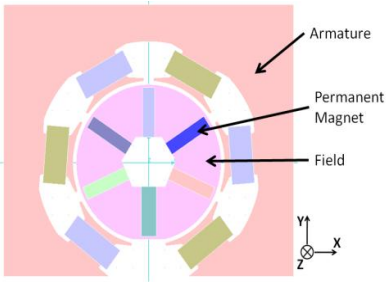

(d) Open type model for long stroke

Figure 6: Fundamental configuration of three-phase units of the proposed model (Significant points in Fig. 6 are marked on the graphs in Fig. 4, Fig. 6 and Fig. 7.).

4 THEORETICAL AND NUMERICAL CALCULATION OF THE PROPOSED MODEL

In the initial design, the authors employed magnetic circuit method in order to estimate characteristics of the proposed model theoretically. And then, the authors analyzed of the proposed model using FEM method

4.1 The air gap flux density

In the proposed model, one armature core consists of six magnetic circuit. In order to estimate characteristics of the proposed model simply, the authors considered one magnetic circuit as shown in Fig. 7(a). Hence, its shape with one magnetic circuit can be changed to equivalent configuration as shown in Fig. 7(b).

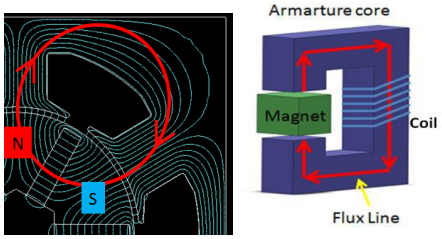

(a) one magnetic circuit (b) Equivalent configuration

Fig. 7: Equivalent configuration considering 1 magnetic circuit

One magnetic circuit in Fig. 5 can be expressed as

$$NI = H_m l_m + 2H_g g_d \text{ [A]} \quad (1)$$

where H_m, H_g is the magnetic-field component of magnet and the air gap, l_m, g_d is the length of magnet and the air gap, I is armature current and N is the winding turn.

If the permeability of armature and field cores is infinite, the maximum magnet flux density B_m in operating point and the maximum air gap flux density B_g can be expressed as (2) and (3).

$$B_m = B_r + \mu_0 H_m \text{ [Wb]} \quad (2)$$

$$B_g = \frac{k_l B_r}{\frac{A_g}{A_m} + 2\frac{g_d}{l_m}}\left(1 - \frac{NI}{H_c l_m}\right) \text{ [T]} \quad (3)$$

In (2) and (3), A_m, A_g is the dimension of magnet and air gap, magnetic-field component of magnet and the air gap, H_c, is the coercive force of magnet, k_l is flux leakage coefficient, B_r is remanence of magnet and μ_0 is permeability of the air gap. Hence, the maximum air gap flux in the proposed model is

$$\emptyset_g = B_g \times 2\pi RL \text{ [Wb]} \quad (4)$$

where R is the length from the center of the field side to air gap, L is the length of magnet to moving direction.

4.2 Back EMF

If the air gap flux is sinusoidal wave, the back EMF and its RMS value can be obtained as (5)

$$e = -p\frac{d\Phi}{dt} = \frac{\pi v}{\tau} N\emptyset_g \sin\left(\frac{\pi v}{\tau} t\right) \text{ [V]}$$

$$E_{rms} = 0.707\frac{\pi v}{\tau} N\emptyset_g \text{ [V]} \quad (5)$$

In (1), Φ is flux in one magnetic circuit, the maximum value of air gap flux, τ is pole pitch, v is the moving velocity, p is the number of pole pairs.
Also, Assuming the condition when d-axis current is controlled to zero, the output of one armature core considered can be expressed as (6). I is a RMS value of the armature current.

$$P = E_{rms} I \quad [\mathrm{W}] \tag{6}$$

4.3 *Detent Force*

From virtual work principle, detent force of one armature core in the proposed model can be expressed as (7).

$$F_{detent} = \frac{k_l^2 B_g^2 RL\pi^2 g_d}{6\mu_0 \tau} \sin\left(\frac{2\pi z}{\tau}\right) \quad [\mathrm{N}] \tag{1}$$

The authors focused on slot-pole combination to reduce detent force. In general, the higher Least Common Multiple (LCM) of slot-pole is, the lower cogging torque can be achieved in the case of rotational synchronous machinery.

Since drive principle of linear synchronous machine is the same with rotational synchronous machine, the authors applied nine slot-eight pole combination to the proposed model in order to reduce detent force and achieve high positioning accuracy in the stage of selecting numbers of armature cores and field poles. Hence, nine armature cores is faced with eight magnets in one electric period as shown in Fig. 6.

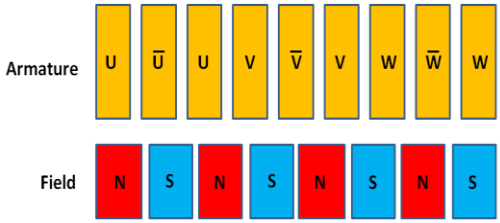

Figure 8: nine slot-eight pole combination.

4.4 *Static Longitudinal Force*

Static longitudinal force of one armature core in the proposed model is

$$F = \frac{k_l^2 B_g^2 RL\pi^2 g_d}{6\mu_0 \tau} \sin\left(\frac{2\pi z}{\tau}\right) + \frac{p\pi v N I k_l \emptyset_{gmax}}{\tau} \sin\left(\frac{\pi z}{\tau}\right) \quad [\mathrm{N}] \tag{2}$$

The first term is detent force expressed in (1) and the second one is thrust of the proposed model. It is found that only detent force exists when I is 0. Also, increasing p in designated dimension results in a decreased pole pitch and thus the thrust will increase, which is one of the advantages of transverse flux type linear motor. Hence, a higher thrust density can be achieved by optimizing p in the proposed model.

The main characteristics based on theoretical values in the proposed model are shown in Table I.

4.5 Evaluation of detent force and static longitudinal force using FEM

In three-dimensional FEM analysis of the proposed model and the reference model, the authors considered three armature cores because it took extensive amount of time to analyze the whole model.

Detent force of the proposed model in three-dimensional FEM analysis is shown in Fig. 8. The maximum value of detent force could be reduced to about 2N when three armature cores moved in one mechanical period which is the distance from point Z1 to point Z2 as shown in Fig. 3 (b) and its wave form was nearly sinusoidal.

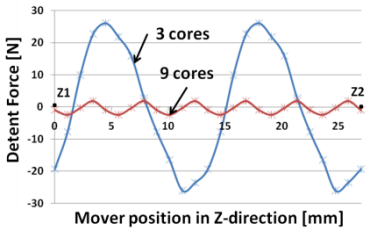

Figure 10: Detent force of the proposed model.

In the case of static longitudinal force, one of the results in I = 5A, N = 50 turns is shown in Fig. 9. The maximum static longitudinal force of the proposed model was 102.3N and that of the reference model in the same condition was 119.2N in one mechanical period.

(a) The proposed model

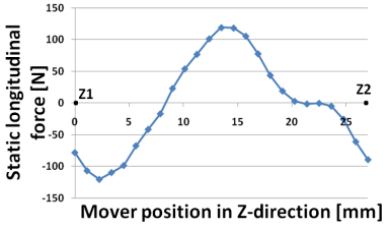

(b) The reference model

Figure 11: Static longitudinal force

The authors expected that a higher static longitudinal force could be obtained because the air gap flux density of the proposed model was higher than that of the reference model in theoretical analysis. However, it was found that thrust of the proposed model would be lower than that of the reference model from the result of three-dimensional analysis. This is because of the flux leakage. This means the strong flux from faced magnets flows into not the air gap but non-magnetic material spacer because of a higher magnetic reluctance of the air outside the field side. Hence, its leaked flux cannot contribute to generate thrust. The flux density distribution in non-magnetic material spacer and of each model is shown in Fig. 7. From the result of the flux density between point Y1 and

point Y2 in Fig. 7, it was found that the amount of flux leaking to non-magnetic material spacer in the proposed model was relatively higher than that in the reference model.

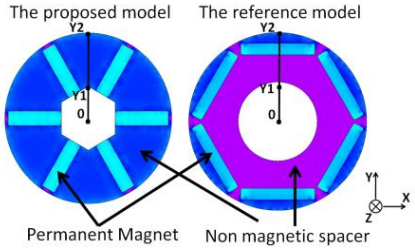

(a) The flux density distribution

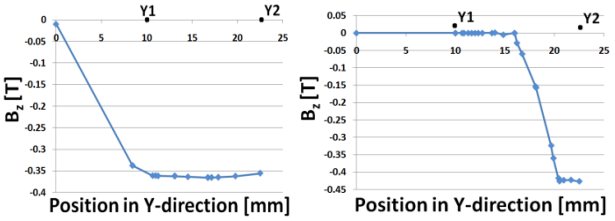

(b) The proposed model (c) The reference model

Figure 7: The flux density in non-magnetic material spacer.

Also, flux distribution without armature core is crucial factor of generating thrust because linear motor is moving by attractive and repulsive force between moving field and the field magnets and not always facing the armature side with the field side like as rotational synchronous machinery. The flux density distribution without the armature side is shown in Fig. 8.

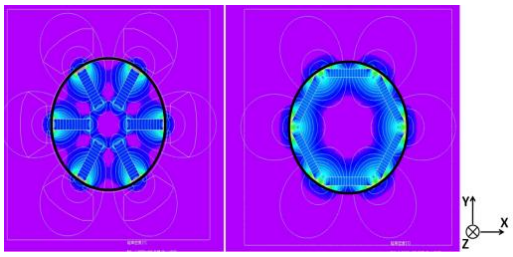

(a) The proposed model (b) The reference model

Figure 8: The flux density distribution without the armature side (The circle is an air gap section.).

When the armature side is located above the field side, the flux from field magnets flows to the armature core because of low magnetic reluctance of the armature core. Also, the air gap flux density of the proposed model and the reference model was respectively 0.7605T and 0.7164T which values are based on three-dimensional FEM analysis. However, as shown in Fig. 8, the flux distribution outside field in the proposed model is lower than that in the reference model. This means attractive force by field magnets laid in front of armature core is low.

Table I the main characteristics of the proposed model

1 armature size [mm]	1 field size [mm]	1 magnet size [mm]
60w× 60h× 7d	20r× 10d	14.3w× 3.8h× 10d
Winding turn N [turns]	Armature current I [A]	Air gap length g_d [mm]
50	5	1.27
Slot-pole combination	Pole pitch τ [mm]	Slot pitch [mm]
9-8	13.5	12
Air gap flux density B_g(max) [T]	*Effective air gap flux density B_g(max) [T]	Flux leakage coefficient k_l
0.92	0.76	0.826
Back EMF E_{rms} [V]	Moving velocity v [m/s]	Output P [W]
7.94	1	39.67

* is based on three-dimensional FEM analysis

5 OPTIMIZATION OF THE FIELD MAGNET CONFIGURATION FOR REDUCING LEAKAGE FLUX

In order to reduce flux leakage and concentrate flux from magnets into the air gap, the authors had to change the configuration of the field magnet. The revised model is shown in Fig. 9.

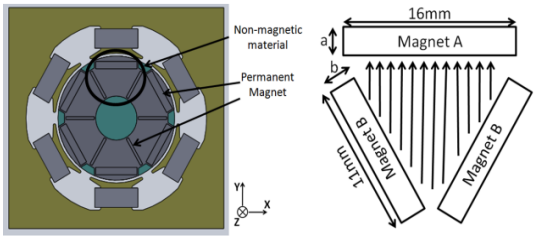

(a) The cross-section (b) Magnetization (Marked on circle in Fig. 9(a))

Figure 9: The revised model

In the revised model, the magnet A in Fig. 9(a), magnet configuration of the reference model is added to the proposed model in order to reduce the flux leakage to non-magnetic spacer.

The width of magnet A and magnet B is 16mm, 11mm respectively considered spatial restriction and structural stiffness but the amount of magnets in one field unit is 2,916 mm^3 the same with the previous model and the reference model.

In order to find the magnet size by varying height a, b in magnet A, B and figure out an effect of static longitudinal thrust by flux-concentration, the authors applied three-dimensional FEM analysis to the revised model. If the total amount of magnet A and magnet B is fixed, b is varying with a under the same amount of magnets and the static longitudinal force is also varying. This result is shown in Fig. 10.

In the case A in Fig. 10(a), width a is 0, i.e the magnet configuration in the proposed model. Also, width b is 0 in the case B which is the magnet configuration in the reference model. From the result considered three armature cores, the maximum static longitudinal force could be increased to 142N when width a and b was 1mm and 0.306mm respectively. Also, the flux density leaking to non-magnetic material spacer was decreased as shown in Fig. 10(b). However, this is mainly considered as the effect of magnet A rather than magnet B. The smaller the

amount of the magnet A is, the smaller static longitudinal force is obtained.

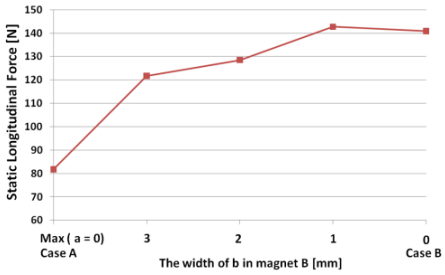

(a) The flux density distribution

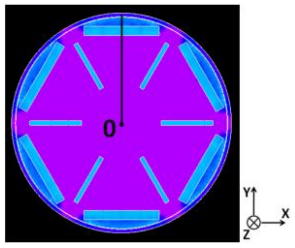

(b) The flux density distribution in non-magnetic material spacer

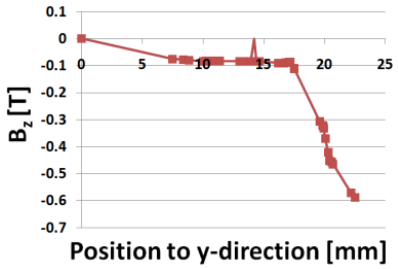

(c) The flux density in non-magnetic material spacer

Figure 10: Static longitudinal thrust by varying magnet width and the flux density in the maximum point.

2 Conclusion

In this paper, a basic structure and the operational principle of the proposed model are described. Also, concept of flux concentrated type field for high thrust is introduced and its characteristics are both theoretically analyzed and numerically computed using finite element method (FEM). By facing magnet each other, magnetic field lines from each magnet are concentrated simply**.** Also, the normal attractive force can be cancelled and design becomes easy by using generic armature cores for brushless DC motor**.**

In FEM analysis, detent force was reduced to about 2N by nine slot-eight pole combination. However, in spite of our initial expectation, a higher thrust was not obtained by the proposed model because of the flux leakage in non-magnetic material spacer. In the revised model, the authors considered the magnet configuration that the reference model is added to the proposed model in order to reduce the flux leakage to non-magnetic spacer.

Although the flux leakage to non-magnetic material spacer could be reduced, the increase of static longitudinal thrust was only 1.4% compared with the reference model. This result could not reach to our initial expectation that higher thrust could be obtained**.** Therefore, it is found that careful design of magnetic circuit for avoiding the flux leakage in cylindrical type linear synchronous motor is important in order to realize the advantages of the proposed idea.

References

[1] Kim H. J, G. S An, J. W Ahn and T. Koseki : “Transverse Flux Type Cylindrical Linear Synchronous Motor for High Thrust using Generic Armature Cores for Rotary Machinery”, IEEJ (In Japanese, reviewing)

[2] W.J. Kim, M.T. Berhan, D.L. Trumper and J.H. Lang : “Analysis and Implementation of a Tubular Motor with Halbach Magnet Array”,1996 IEEE-IAS Annual Meeting, SanDiego, CA, October 5-10 (1996)

[3] Weh. H, Hoffman. H, Landrath. J : “New Permanent Magnet Excited Synchronous Machine with High Efficiency at Low Speeds”, Proceedings of the International Conference on Electrical Machines, 1988.

[4] T. Kenjo, S. Nagamori : “Brushless motors : advanced theory and modern applications”, Sogo Electronics Press, 2003.